Electronic Supplementary Information (ESI)

An efficient heteroatom-doped carbon electro-catalyst for oxygen reduction reaction by pyrolysis of protein-rich pulse flour cooked with SiO_2 nanoparticles

Rohan Gokhale,[a] Sreekuttan M. Unni,[a] Dhanya Puthusseri,[a] Sreekumar Kurungot*[a] and Satishchandra Ogale*[a]

[a] *Physical and Materials Chemistry Department, National Chemical Laboratory (CSIR), Dr. Homi Bhabha Road, Pune-411008, India*

ESI-I

TABLE S1

No.	Reference	Material	Onset Potential of Material (V) with loading	Onset Potential (V) of commer. Pt/C ref used with loading	Electrolyte used	Ave. No. of elec. transferred	Reference Electrode used
1	Jeon et al. *J. Am. Chem. Soc.* **2013**, 135, 1386−1393	Acid functionalized GNPs	-0.16 (5µl of 1mg/ml dispersion of catalyst)	0.5 (Similar procedure used to drop cast)	0.1 M KOH	2.6-3.6	Ag/AgCl
2	Li et al. *J. Am. Chem. Soc.* **2012**, 134, 18932−18935	N-doped colloidal graphene quantum dots	0.04, 0.10 and 0.14 V negative to reference Pt/C (15 µg on GCE)	Not mentioned (15 µg on GCE) 20% wt. Pt on Vulcan XC-72R	0.1 M KOH	3.9	SCE
3	Yang et al. *J. Am. Chem. Soc.* **2012**, 134, 16127−16130	Phosphorus doped ordered mesoporous carbon	-0.11	Not mentioned (20 wt % Pt supported on Vulcan XC72R carbon	0.1 M KOH	3.9	Ag/AgCl
4	Wohlgemuth et al. *J. Mater. Chem. A*, **2013**, 1, 4002–4009	N doped carbon aerogels	Not precisely defined but significantly negative to platinum. 5 µl of 5 mg/350 µl	Not mentioned 20 wt% Pt@C	0.1 M KOH	3.3	Ag/AgCl
5	Zhang et al. *Adv. Mater.* **2013**, *25*, 4932–4937	Phosphorus doped graphene	0.92 10 µ L of 1mg/mL solution	0.95 10 µ L of 1mg/mL solution	0.1 M KOH	3-3.8	RHE
6	Wang et al. *Angew. Chem. Int. Ed.* **2012**, 51, 4209 –4212	Boron and Nitrogen doped CNTs	Not precisely defined but shown to be comparable to platinum. 10 µ L of 1mg/mL solution	Not defined precisely 20% platinum on Vulcan XC-72R; E-TEK	0.1 M KOH	Close to 4	SCE
7	Silva et al. *J. Am. Chem. Soc.* **2013**, 135, 7823−7826	N and O doped mesoporous carbon	0.94 (100 µg/cm^2)	Not precisely mentioned but graph shows comparable behavior Pt/C (1% Pt)	0.1 M KOH	~4	RHE
8	Chen et al. *Adv. Mater.* **2012**, *24*, 5593–5597	N doped carbon nanocages	-0.13 10 µ L of 2mg/mL solution	-0.03 10 µ L of 2mg/mL solution Pt/C (with Pt loading of 20%,	0.1 M KOH	3.27	Ag/AgCl

9	Lin et al. *Adv. Energy Mater.* **2012**, *2*, 884–888	N doped Graphene	-0.1 141 μ g cm $^{-2}$	No comparison shown Pt/C (20 wt.% Pt)	0.1 M KOH	3.6	Ag/AgCl
10	Liang et al. *Angew. Chem. Int. Ed.* **2012**, 51, 11496 –11500	S,N doped mesoporous Graphene	-0.06 10 μ L of 2 mg/mL solution	-0.03 20 wt% Vulcan Pt/C	0.1 M KOH	3.6	Ag/AgCl
11	Liu et al. Nano Res. **2013** DOI 10.1007/s12274-013-0307-9	N doped nanoporous carbon	0.88 (0.1mg/cm^2)	- (0.1mg/cm^2) Pt/C (20 wt.% Pt loading	0.1 M KOH	~4	RHE
12	Yang et al. *J. Am. Chem. Soc.* 2011, *133*, 206–209	N doped mesoporous carbon	0.035	0.06 20 wt% Pt/C (130 μg loading)	0.1M KOH	~3-4	Ag/AgCl
13	Gong et al., Science 2009, 323,760-763	N doped VA-CNTs	Observed around 0 V (Not mentioned precisely)	Observed around 0 V (Not mentioned precisely)	0.1 M KOH	3.9	Ag/AgCl
14	**Our Work**	**N doped heirarchically porous carbon**	**0.949 (255μg/cm^2)**	**0.972 (25 μg/cm^2) Pt/C (20 wt.%)**	**0.1 M KOH**	**3.5**	**RHE**

Synthesis Protocols of the materials for the references given above:

1. "Edge-selectively functionalized graphene nanoplatelets (EFGnPs) with different functional groups were efficiently prepared simply by dry ball milling graphite in the presence of hydrogen, carbon dioxide, sulfur trioxide, or carbon dioxide/sulfur trioxide mixture"- Jeon et al. *J. Am. Chem. Soc.* **2013**, 135, 1386−1393

2. "Solution chemistry approach to nitrogen-doped colloidal graphene quantum dots with well-defined structures" - Li et al. *J. Am. Chem. Soc.* **2012**, 134, 18932−18935

3. "Phosphorus-doped ordered mesoporous carbons (POMCs) with different lengths were synthesized using a metal-free nanocasting method of SBA-15 mesoporous silica with different sizes as template and triphenylphosphine and phenol as phosphorus and carbon sources, respectively". HF was used for etching subsequently. Yang et al. *J. Am. Chem. Soc.* **2012**, 134, 16127−16130

4. "A one pot hydrothermal synthesis towards nitrogen doped organic aerogels with tunable surface area and nitrogen content is presented. The gels were synthesized from a sustainable glucose carbon precursor with 2-pyrrol-carboxaldehyde (PCA) as the nitrogen source and borax mineral as the structure forming agent." Wohlgemuth et al. *J. Mater. Chem. A*, **2013**, 1, 4002–4009

5. "A facile, low-cost and scalable thermal annealing method for the synthesis of PG using graphite oxide (GO) and triphenylphosphine (TPP) as carbon and phosphorus sources, respectively"- Zhang et al. *Adv. Mater.* **2013**, *25*, 4932–4937

6. "Developed a facile approach to metal-free BCN graphene of tunable B/N co-doping levels as efficient ORR electrocatalysts simply by thermal annealing GO in the presence of boric acid and ammonia" Wang et al. *Angew. Chem. Int. Ed.* **2012**, 51, 4209 –4212

7. "Mesoporous oxygen- and nitrogen-doped carbons were synthesized from in situ polymerized mesoporous silica-supported polyaniline (PANI) by carbonization of the latter, followed by etching away the mesoporous silica template from it." Silva et al. *J. Am. Chem. Soc.* **2013**, 135, 7823−7826

8. "NCNCs were prepared with pyridine as the precursor in this study". MgO was used as a template - Chen et al. *Adv. Mater.* **2012**, *24*, 5593–5597

9. GO was treated with SiO_2 nanoparticle solution and then dual doped using chemicals like BDS/Melamine (heat treatment). HF was used for etching. Liang et al. *Angew. Chem. Int. Ed.* **2012**, 51, 11496 –11500

10. "N-doped porous carbon materials have been prepared by a simple one-step pyrolysis of ethylenediaminetetraacetic acid (EDTA) and melamine in the presence of KOH and Co(NO3)2·6H2O."- Liu et al. Nano Res. **2013,** DOI 10.1007/s12274-013-0307-9

11. "NG is successfully prepared from GO and a solid N precursor, urea, both of which are low-cost and being manufactured in large quantities." "Well-mixed GO and urea were pyrolyzed at 800 ° C in an inert environment" - Lin et al. *Adv. Energy Mater.* **2012**, *2*, 884–888

14. In our work, the protein enriched food grain powder (gram flour, soyabin) was cooked with SiO_2 nano-particle dispersion in water (Ludox). During swelling of the grain matrix SiO_2 nanoparticles were uniformly sucked-in and distributed. After SiO_2 etching by HF hierarchically porous nitrogen doped conducting carbon was obtained which gave a good ORR performance.

ESI-II

Characterizations:

Field Emission Scanning Electron Microscopy (FESEM, Nova NanoSEM 450) and High Resolution-Transmission Electron Microscopy (HR-TEM, FEI Tecnai 300) were used. The surface area of carbon was obtained from BET surface area measurements (Quantachrome Quadrasorb automatic volumetric instrument). X-ray photoelectron spectroscopy (XPS) (ESCA-3000, VG Scientific Ltd. UK, with a 9 channeltron CLAM4 analyzer under vacuum better than 1* 10^{-8} Torr, Al Ka radiation (1486.6 eV) and a constant pass energy of 50 eV) was employed to study the chemical state of carbon in the materials respectively. X-ray Diffraction (XRD, Philips X'Pert PRO) and Raman spectroscopy (a confocal micro-Raman spectrometer LabRAM ARAMIS Horiba JobinYvon, with laser excitation wavelength of 612 nm) was also used.

Resistance Measurement:

5 mg of each carbon catalyst was mixed with 1 mg of binder (kiner). 1 ml NMP was added and the contents were ground in a mortar pestle to make a uniform thin paste. 7 µL of the paste was drop casted on 0.5* 0.5 cm of glass slide. Resistance was measured over a distance of 1 mm on a two-probe system.

Electrochemical studies: Biologic electrochemical workstation was used for all electrochemical analysis with conventional three- electrode test cell from Pine Instruments. Hg/HgO and graphite rode were used as the reference and counter electrodes, respectively. A glassy carbon (GC) electrode (5 mm diameter) embedded in Teflon was used as working electrode. Working electrode was polished using 0.3 μm alumina slurry and cleaned using water and alcohol. 10 mg of the catalyst was dispersed in 2 ml of dimethyl acetamide by ultrasonication. 10 μL from the prepared slurry was drop casted on the GC electrode followed by coating of 2 μL of 0.1 %

Nafion® solution. Cyclic voltammetric (CV), chronoamperometric (CA) and rotating disc electrode (RDE) studies were carried in 0.1 M KOH (Aldrich). 5 mV s^{-1} scan rate was used for both RDE and cyclic voltammetric analysis. For RDE analysis, oxygen and nitrogen saturated 0.1 KOH was used respectively for oxygen saturated and oxygen free environment.

For Rotating ring disc electrode (RRDE), carbon samples (50µl) coated on 0.24 cm^2 glassy carbon disc surrounded by platinum ring were used as working electrode and Hg/HgO and graphite rode were used as reference and counter electrode respectively. Oxygen saturated 0.1 M KOH was used for RRDE analysis. All potentials were converted to RHE by calibrating Hg/HgO in hydrogen saturated 0.1 M KOH.

ESI-III

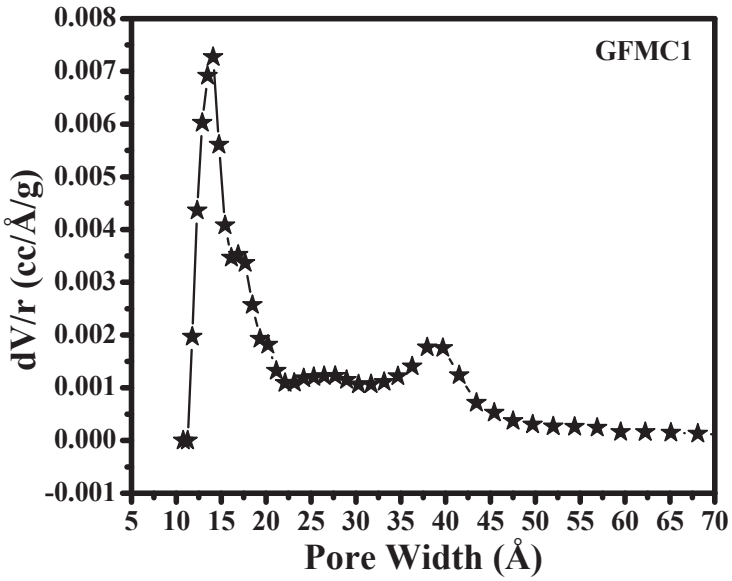

Figure S1. Pore size distribution of GFMC1

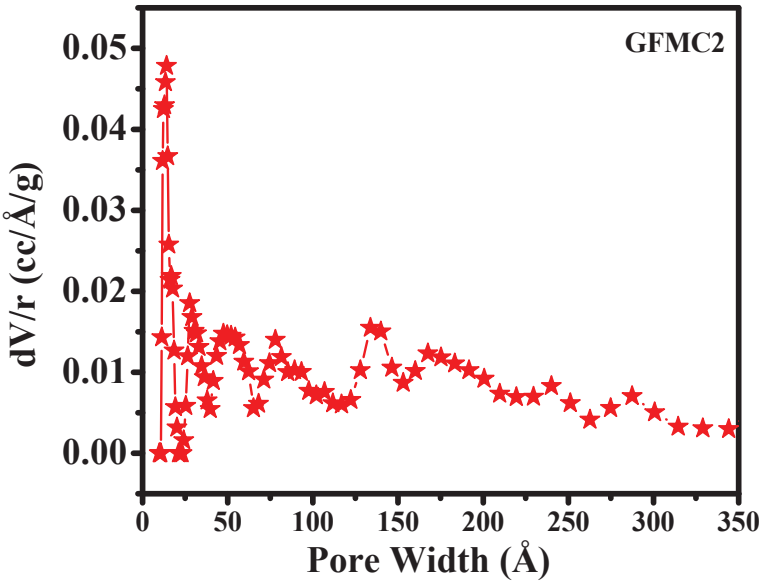

Figure S2. Pore size distribution of GFMC2

ESI-IV

Adsorption isotherms for GFMCs

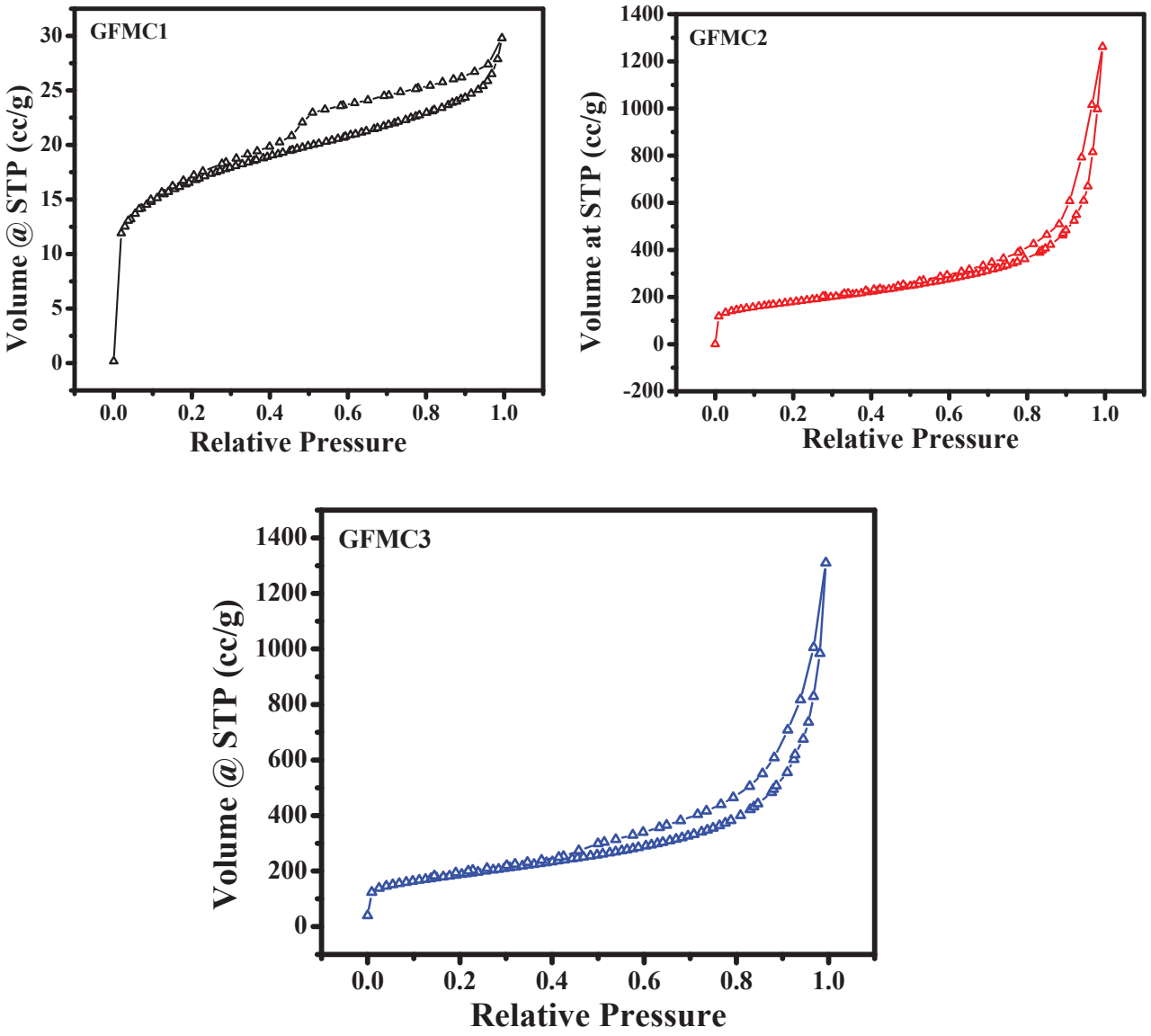

Figure S3. Adsorption isotherms for GFMCs

All the samples were measured by nitrogen adsorption–desorption experiments at 77 K. All the adsorption isotherms are of type II with typical hysteris loop at high value of p/p^0. Hysteresis loop at high value of p/p^0 signifies microporosity in these materials.

ESI-V

Table S2. Atomic Percentages for GFMCs

Material	C	N	O
GMFC1	73.26	1	25.73
GMFC2	84.77	0.75	14.47
GMFC3	88.81	1	10.23

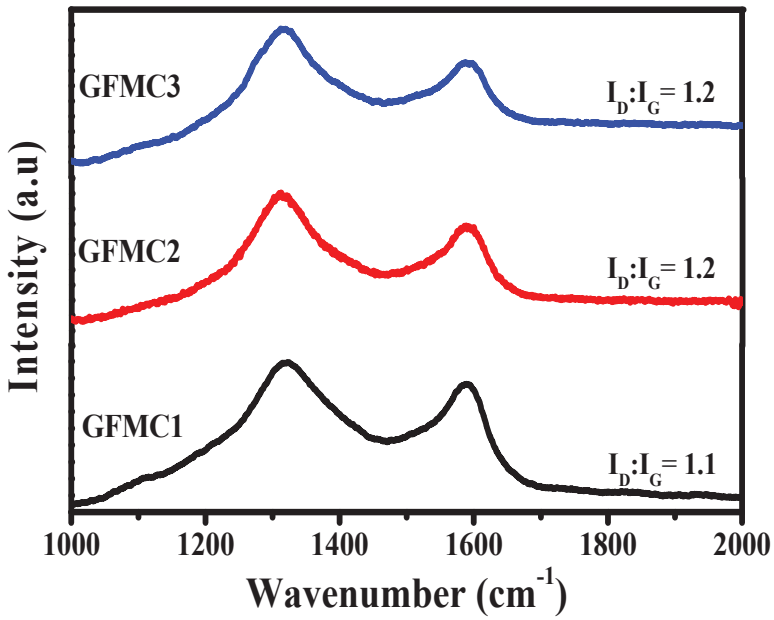

Fig S4. Raman Spectroscopy of GFMCs

Raman spectroscopy of the GFMCs reveal the characteristic D band of carbon at 1315 cm^{-1} and G band due to sp^2 carbon 1590 cm^{-1}. The I_D: I_G ratio shows an expected increase in the porous GFMC2 and GFMC3 as compared to GFMC1 due to the increase in number of defects in the systems.

ESI-VI

Conversion of Hg/HgO to RHE

Hg/HgO electrode calibration was carried in a three electrode system with Pt wires as working and counter electrode and Hg/HgO as reference electrode. Hydrogen saturated 0.1 M KOH was used as an electrolyte. Linear sweep voltammetry was performed at 1 mV/s scan rate and the potential at which current crosses zero was taken as thermodynamic potential (vs Hg/HgO) for the hydrogen electrode.

The potential at which current crosses zero is -0.949V vs Hg/HgO

So E (RHE) = E (Hg/HgO) + 0.949

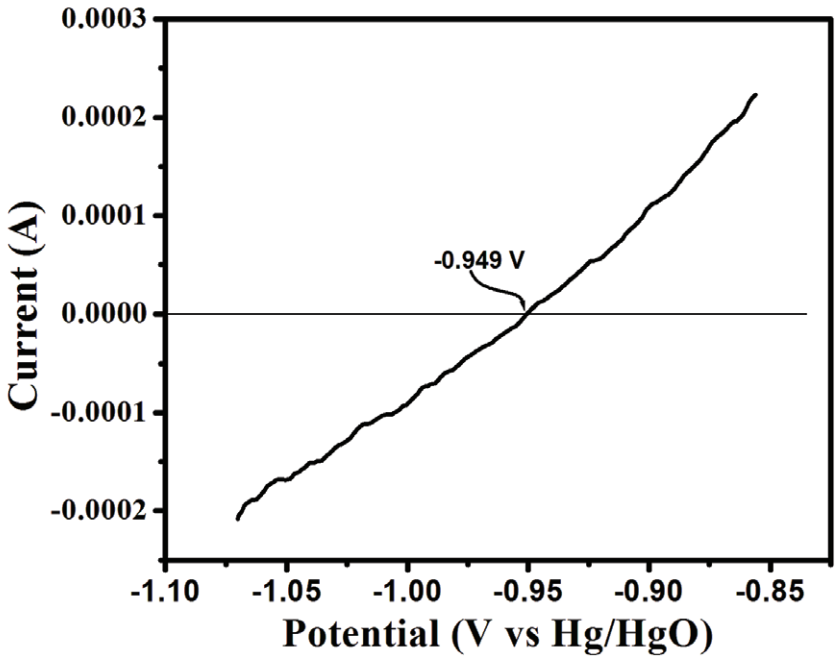

Figure S5. Calibration curve for reference electrode

ESI-VII

LSV curves of all GFMC at different electrode rotation

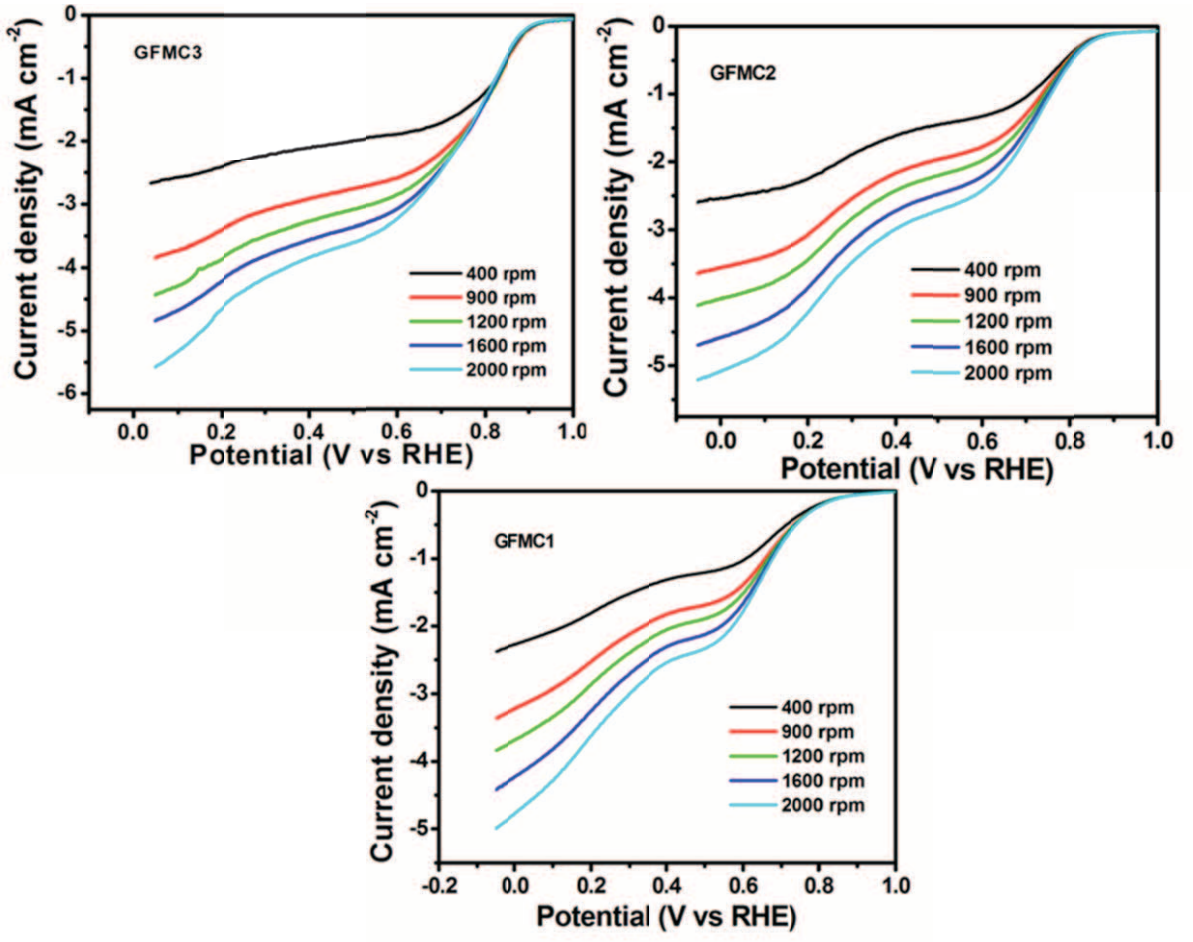

Fig S7. *Linear sweep voltammograms of GFMCs at different rotation in an oxygen saturated 0.1M KOH with a scan rate of 5 mV* s^{-1} .

ESI-VIII

Details of commercial Pt/C (20%) used for the comparison of electrochemical performance

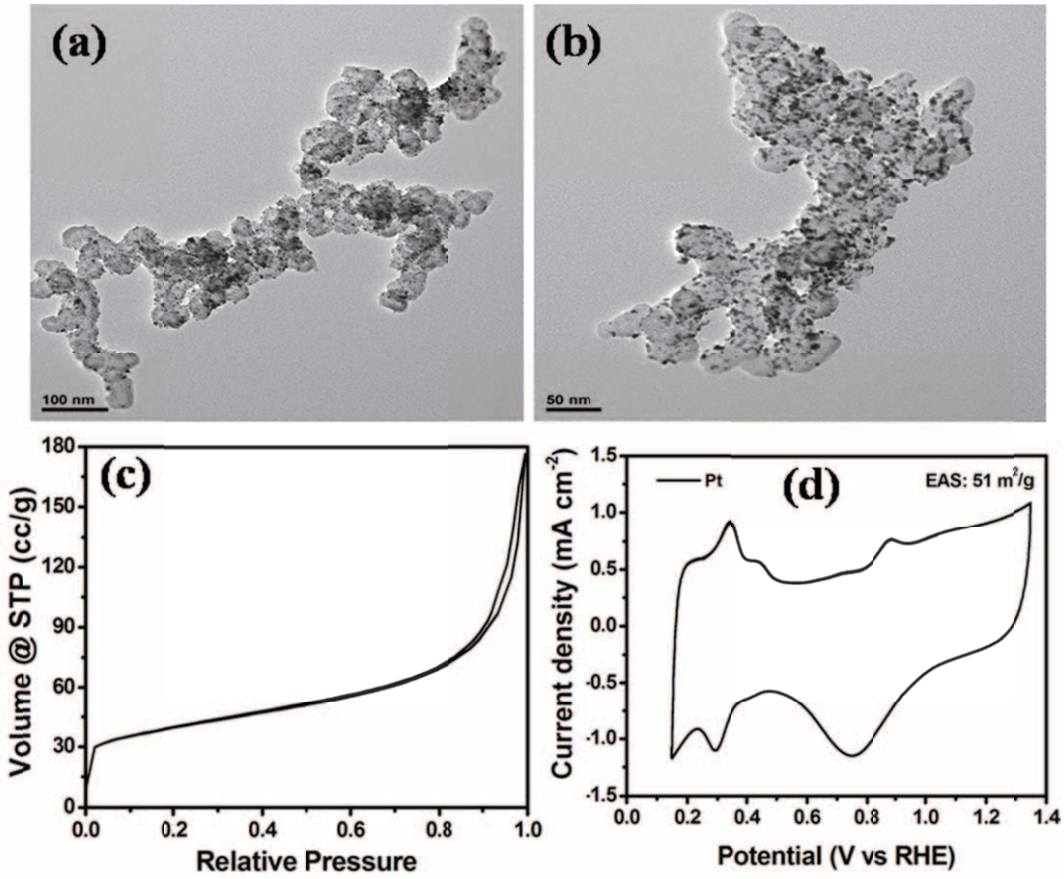

Figure S6: (a) & (b) are the TEM images of Pt/C at different magnification. Pt particle size is varying in between 3 - 5 nm (c) N_2 adsorption isotherm of Pt/C. Calculated BET surface area is 130 m^2/g (d) Cyclic voltammogram of Pt/C at 50 mV/s scan rate in 0.1 M KOH solution. Electrochemical active surface was calculated from the hydrogen desorption area of the voltammogram and it is 51 m^2/g. (Pt loading in the electrode is 25 µg/ cm^2 and area of electrode is 0.196 cm^2).

ESI- IX

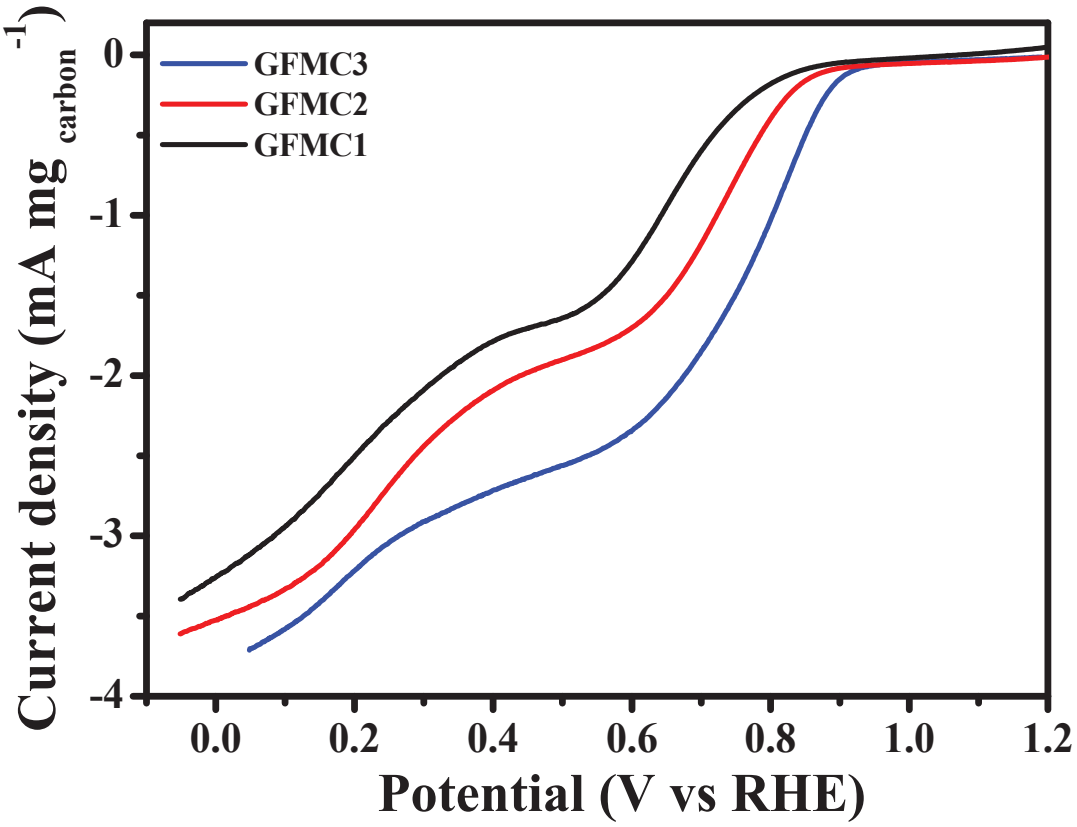

Fig S8. Current Density of the catalysts plotted in terms of mA/mg a) Pt/C b) GFMCs

ESI- X

Onset potential determination

The potential where the reduction current sharply increasing compared to blank is considered as the onset potential for the ORR. (LSV in oxygen saturated 0.1 M KOH at 1600 rpm is given in black and LSV in nitrogen saturated 0.1 M KOH at 0 rpm as blank in red)

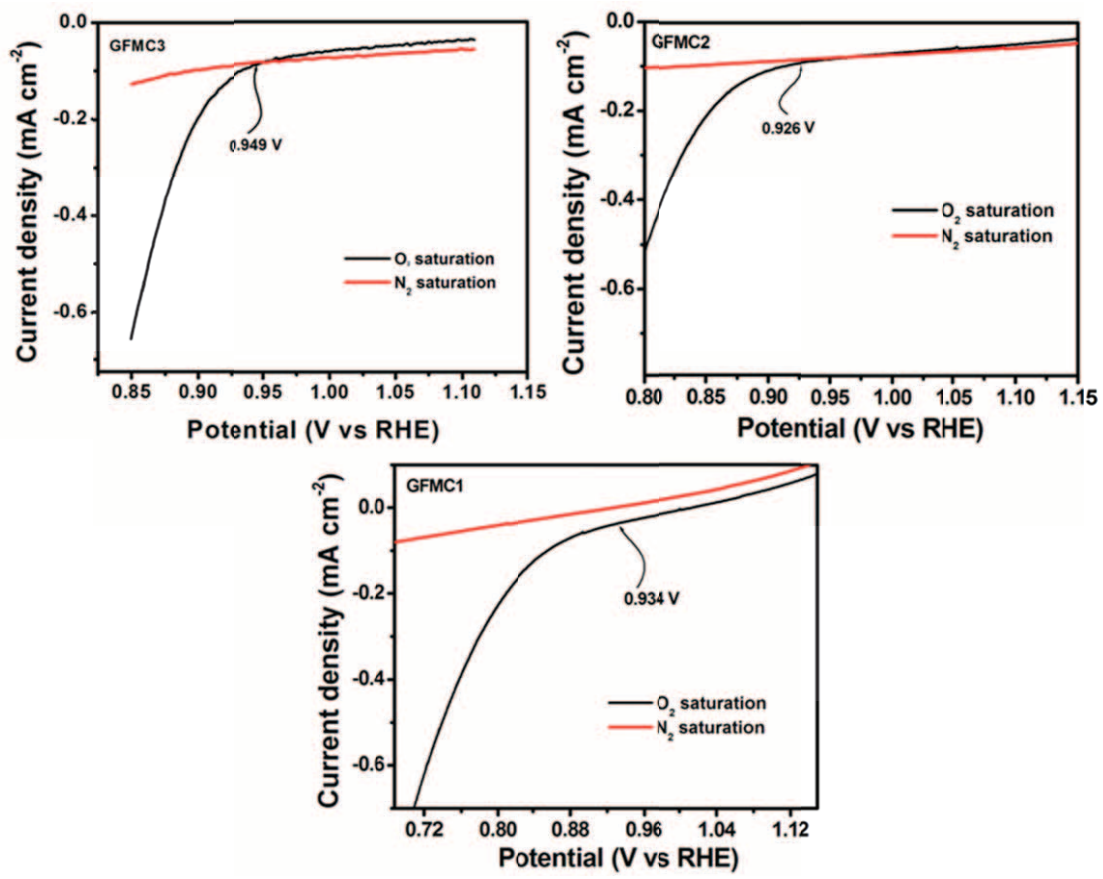

Fig S9. *Linear sweep voltammogram of GFMC at rotation at 1600 rpm in an oxygen saturated 0.1M KOH with a scan rate of 5 mV s^{-1} (Black) and in nitrogen saturated 0.1 M KOH at zero rotation (Red).*

ESI XI

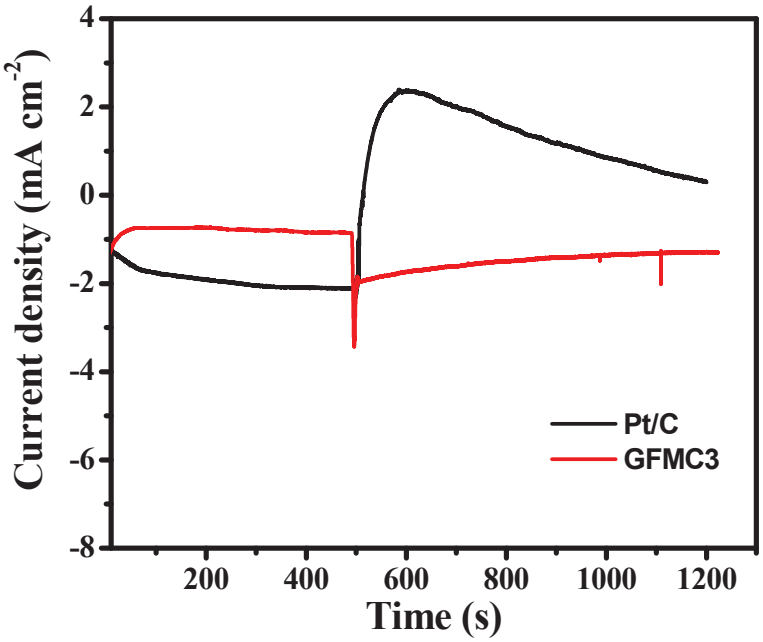

Fig S10. *Methanol tolerance studies of GFMC3 at a rotation speed of 1000 rpm in oxygen saturated 0.1 M KOH at 0.8 V. At 500 s, 3 M methanol was added into the electrolyte in order to evaluate the crossover effect.*

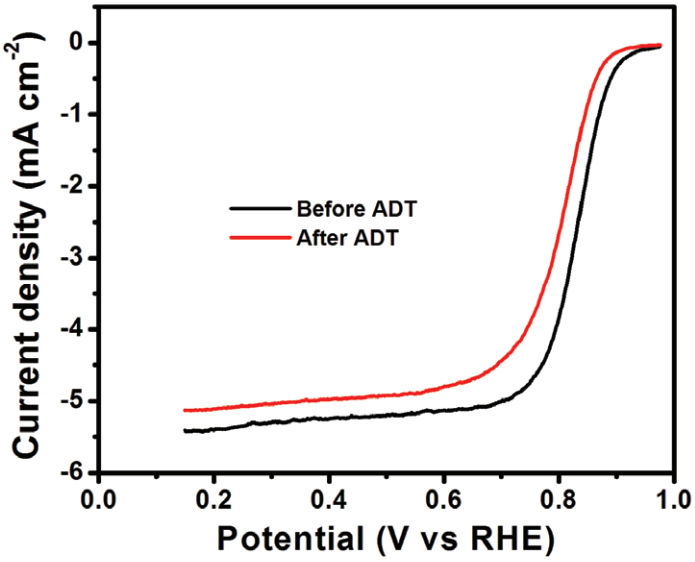

Fig S11. *Linear sweep voltammogram of a) Pt/C catalyst at rotation of 1600rpm in an oxygen saturated 0.1M KOH with a scan rate of 5 mV s^{-1} before and after 5000 potential cycling (Accelerated Durability Test (ADT)).* ***Note:*** *The LSV curves for Pt/C in Figure 7 and Figure S12 are slightly different as compared to the curve given here. This is because for this ADT*

experiment we had to use the catalyst material from a different batch, having exhausted with the materials we had before. The LSV curves of Figure 7 and Figure S12 are the same.

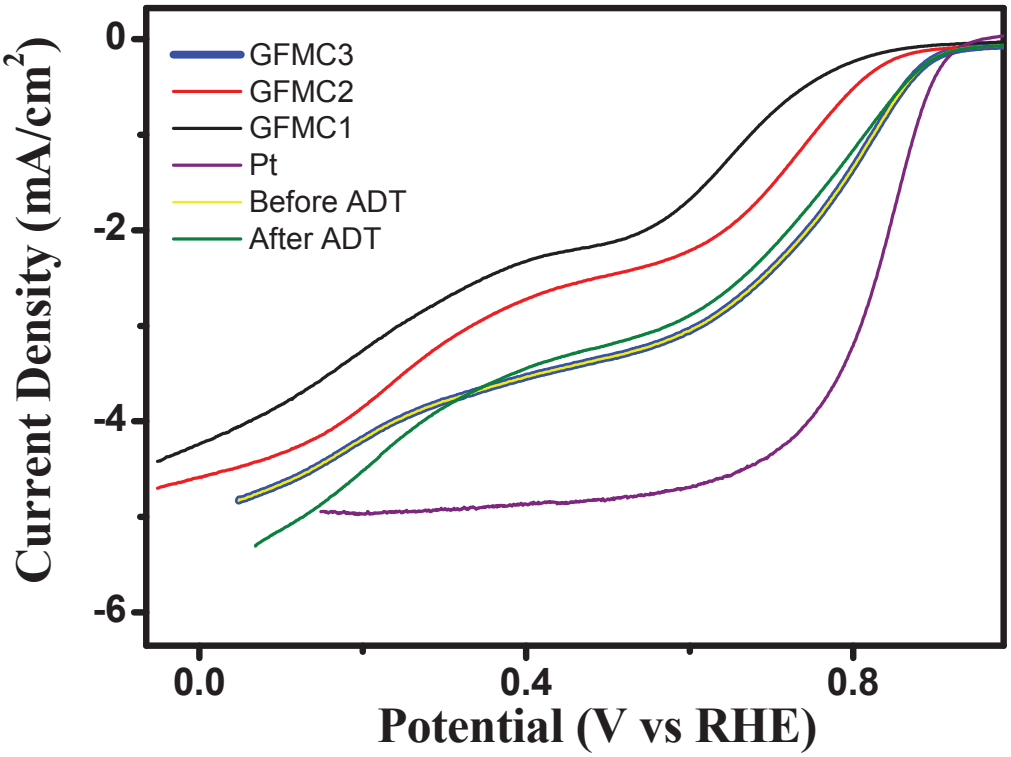

Fig S12. ADT plot of GFMC3 plotted with the LSV of the GFMCs

ESI-XII

SBMC1 as an electrocatalyst for ORR

XPS analysis shows that SBMC1 contains Carbon, Nitrogen and Oxygen in the ratio of 22:1.25:80. Very high oxygen content is observed in this material. A slightly greater % N atom doping (1.25%) is seen in SBMC1. This may be due to increased protein content of the precursor. The nitrogen content shows peaks at 399.7 eV (pyrrolic N), 401.3 eV (graphitic N), 403.3 eV (oxygenated N) (Fig S5)

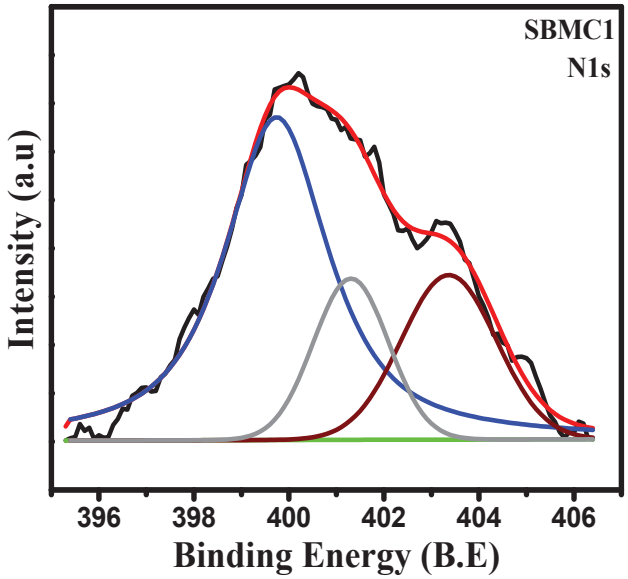

Fig S13. *XPS analysis of N1s in SBMC1*

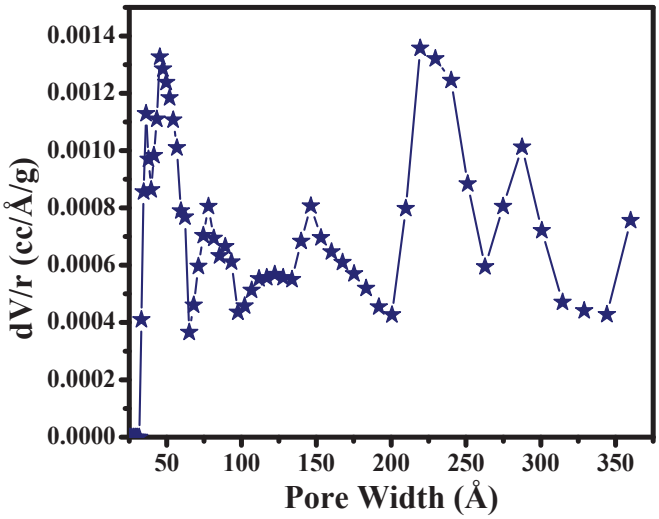

Fig S14. *Pore size distribution of SBMC1*

The pore size distribution of SBMC1 shows a similar hierarchical pore distribution which is responsible for enhanced catalytic activity (Fig S14). The BET surface area of SBMC1 however is low (28 m^2/g).

This could be due to insufficient penetration of SiO_2 nanoparticles into the seed coat of soybean grains during the synthesis. The resistance of SBMC1 pellet also shows an increase as compared to GFMCs (~ 10.23 ohms). However the good performance in ORR in this case can be attributed to an increased nitrogen doping percentage and oxygen functionalization as compared to GFMCs. It is quite clear that SBMC1 possesses large number of catalytic sites inspite of having lesser surface area and conductivity as compared to GFMC2.

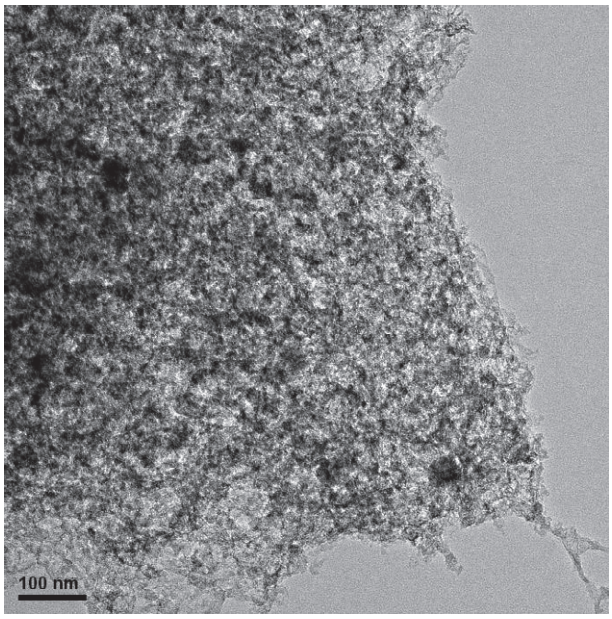

Fig S15. *TEM image of SBMC1*

Electrochemical Properties

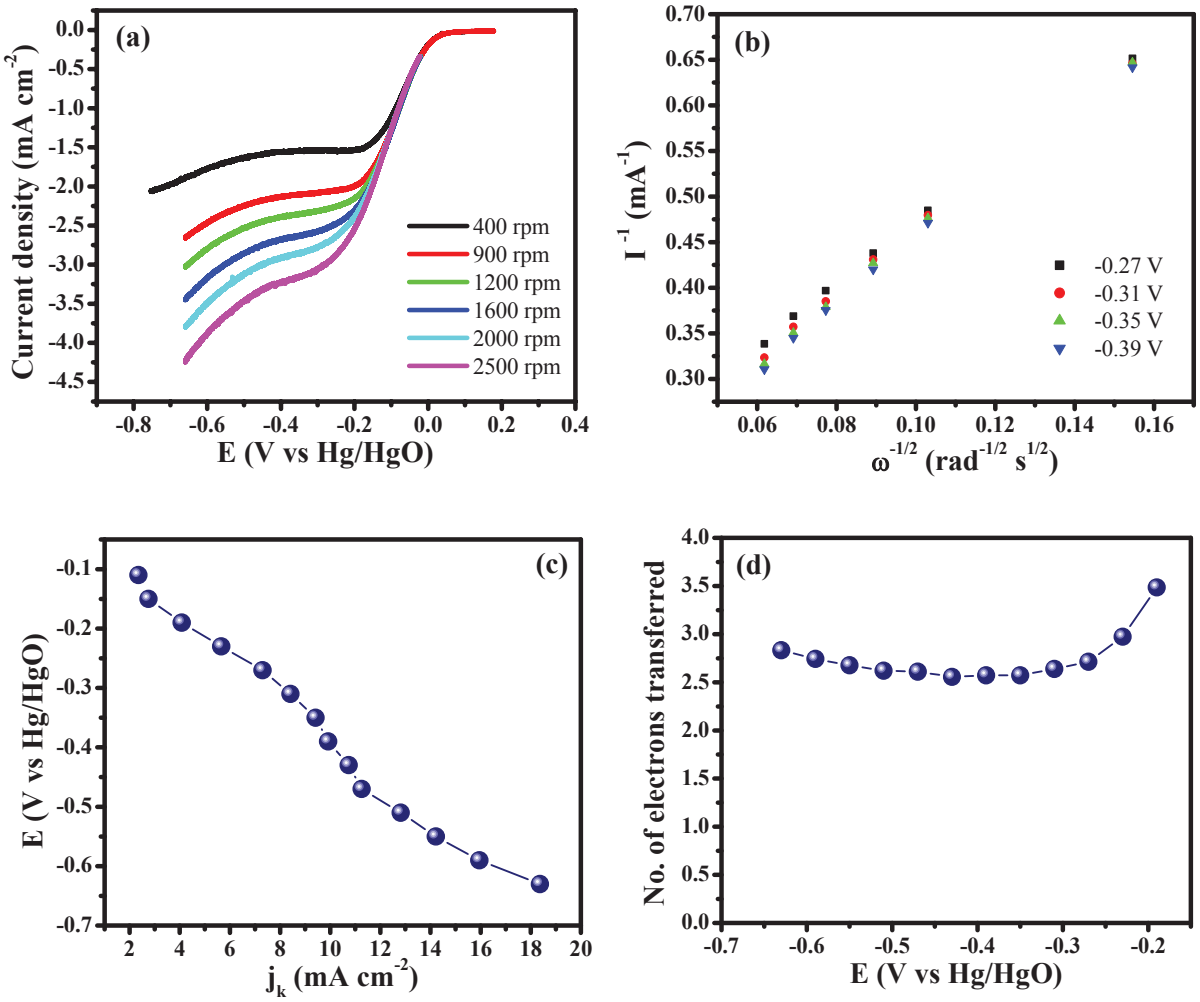

Fig S16. *a) LSV studies of the SBMC1 catalysts in 0.1 M oxygen saturated KOH at different electrode rotation with scan rate is 5 mV s^{-1}. Reference electrode is Hg/HgO and graphite rode as counter electrode. b) K-L plots of the SBMC1 at different potential. Plots are derived from the LSV at different rotation speed. c) Kinetic current density of the GFMCs Calculated from the slope of K-L plot d) Number of electron transfer calculated from the slope of K-L plot.*

Figure S16 a, shows LSV curves of SBMC1 at different rotation speed with an onset potential of 0.05 V vs Hg/HgO for ORR. SBMC1 also showing excellent ORR activity similar to GFMCs. SBMC1 shows ORR electron transfer number around 3 in the entire potential range. This clearly indicates that SBMC1 follow a mixed kinetics where both peroxide and OH- formation occurs. Electrocatalytic activity of SBMC1 proves pyrolysis of protein enriched food waste is a generalized strategy to synthesize cost effective fuel cell electrocatalyst for ORR.